

Supporting Information

Fish scales inspired design of underwater superoleophobic microcones arrays by sucrose solution assisted femtosecond laser irradiation for multifunctional liquid manipulation

*Guoqiang Li,^a Yang Lu,^b Peichao Wu,^a Zhen Zhang,^a Jiawen Li,^{*a} Wulin Zhu,^a Yanlei Hu,^a Dong Wu,^{**a} and Jiaru Chu^a*

^a Micro/Nano Engineering Laboratory, University of Science and Technology of China, Hefei, Anhui, 230026, PR China.

^b Precision and Equipment Support Laboratory, Department of Instrument Science & Opto-Electronics Engineering, Hefei University of Technology, Hefei, Anhui, 230009, PR China.

E-mail: jwl@ustc.edu.cn and dongwu@ustc.edu.cn

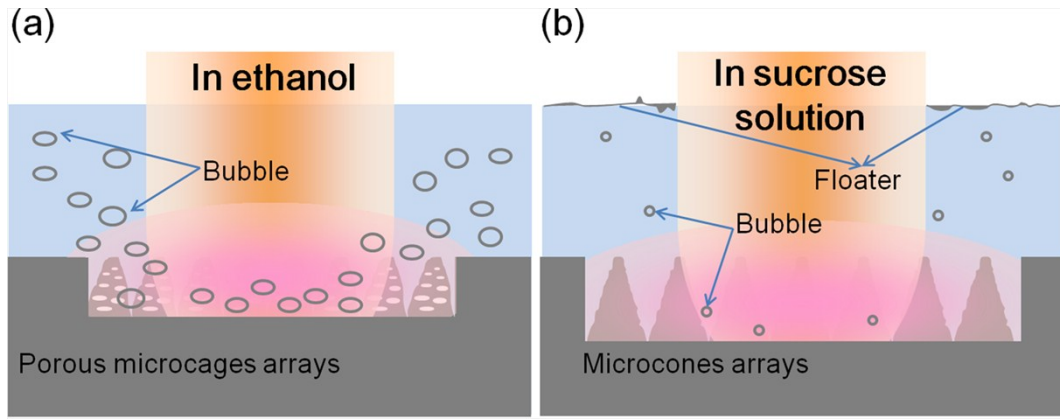


Figure S1. The comparison of experimental phenomena for preparing porous microcages arrays in ethanol and microcones arrays in sucrose solution. (a) The schematic diagram of preparing porous microcages arrays in ethanol. In experiments, it is found that many bubbles are formed during the laser irradiation due to the low boiling point of ethanol. The micro-explosion of the bubbles leads to the formation of the porous micro/nanocages arrays. However, in sucrose solution, there are few tiny bubbles generated and hardly any micro-explosion phenomenon due to the high viscosity of sucrose, which contributes to the formation of microcones arrays. Additionally, different from the irradiation in ethanol, the floaters consisting of bubbles and particulate matters are produced and float on the solution.

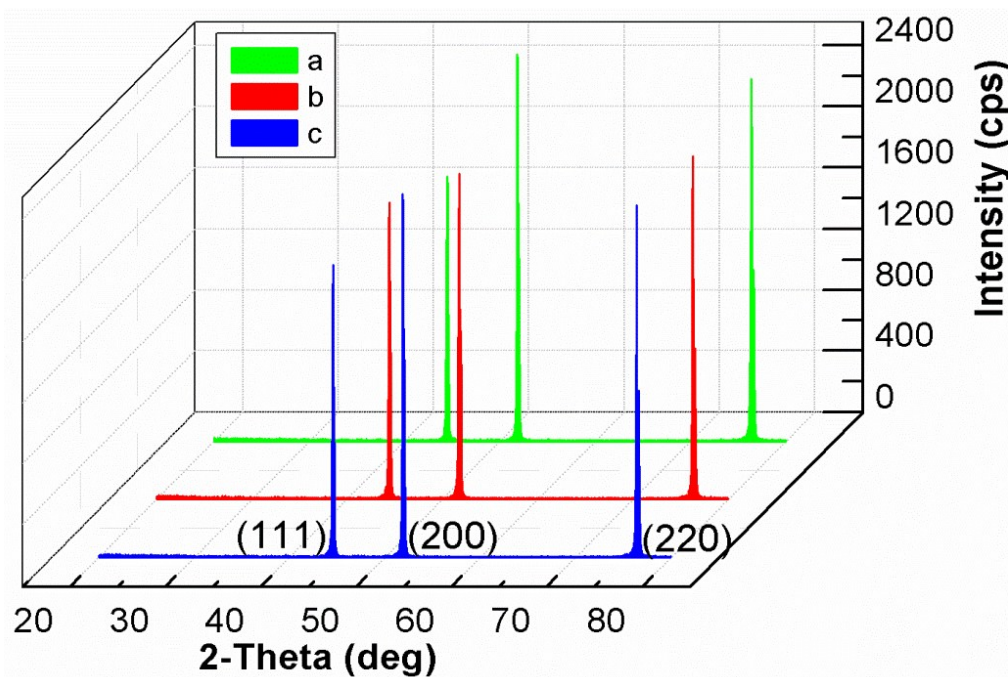


Figure S2. The XRD analysis of the chemical component of the nickel processed in sucrose solution. a, b denote XRD curves of nickel processed in mass ratio of 10:100, under pulse energy of 0.10 and 0.19 mJ, respectively. C indicates that the XRD results as a function of mass ratio of 55:100, pulse energy of 0.10 mJ. It is observed that the peaks appear at 44.5°, 51.8°, and 76.4°, which mean the positions for Ni. From the XRD curves, there is no other peak seen. Combined with the XRD analysis in the paper, the measurement covers the minimal and maximal mass ratio and pulse energy, which can certify powerfully that no chemical changes happen in sucrose solution.

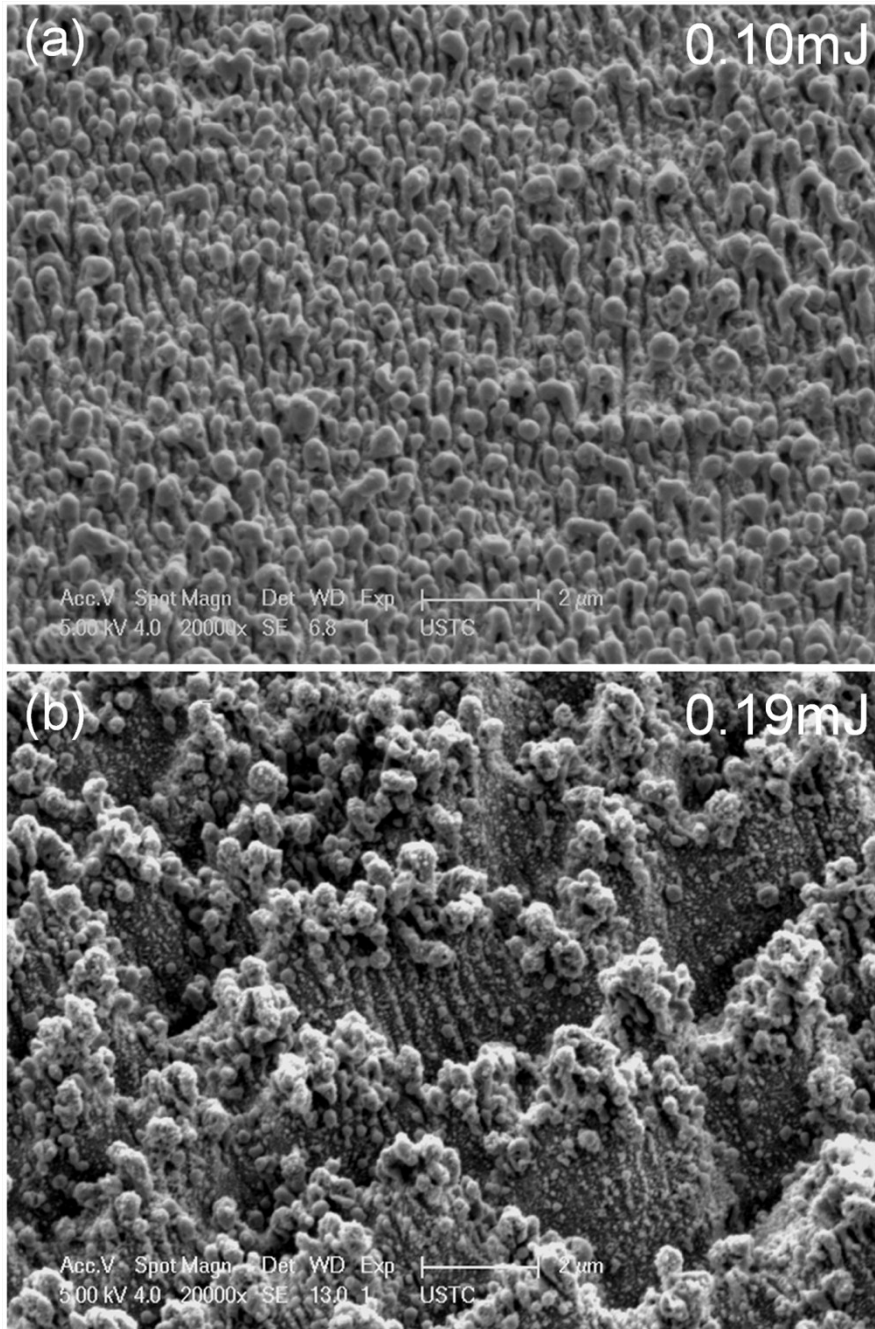


Figure S3. The SEM images of nickel surfaces processed in sucrose solution with mass ratio of 5:100. (a) The surface treated under pulse energy of 0.10 mJ. It can be seen that the surface is covered by particles with size from tens to hundreds nanometers, and no cone was formed. (b) The surface prepared under 0.19 mJ. Under this condition, there is still no cone generated, but only uneven ravine-like structures covered by nanoparticles formed on the processing area. This results show that under the mass ratio of 10:100, there is no cone structures can be prepared.

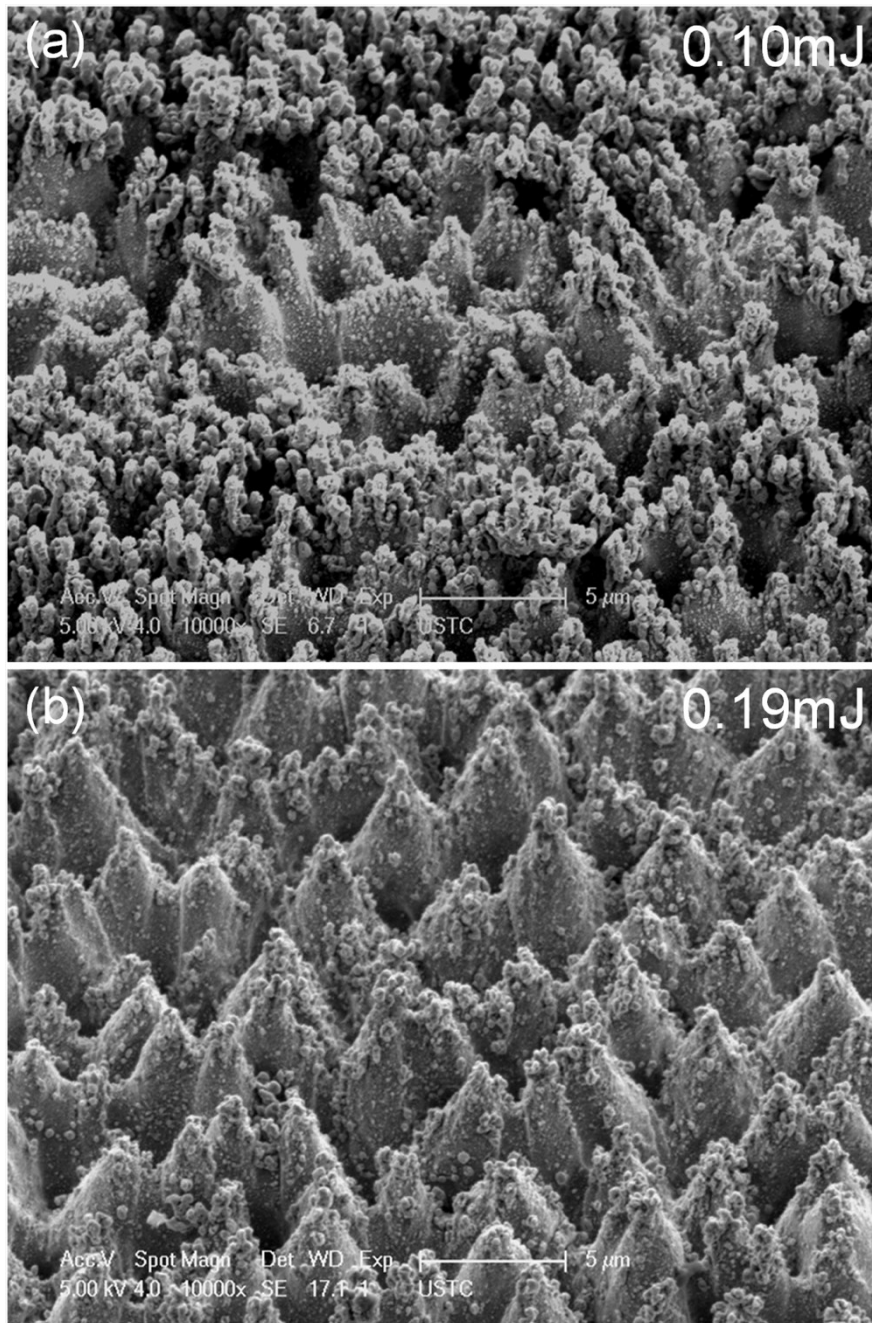


Figure S4. The SEM images of nickel surfaces processed in sucrose solution with mass ratio of 75:100. (a) The surface morphology of nickel prepared under pulse energy of 0.10 mJ. In this case, although few irregular cones are formed, there are plenty of various nanoparticles generated around the formed cones, and covered them completely. (b) The cones formed under the pulse energy of 0.19 mJ. It is indicated that the cones appear on the whole processing area. However, not only the height and size are decreased compared with the good cones mentioned in the paper, but also they are very heterogeneous, showing weak

controllability. In addition, the top of the cones are covered with several to tens of nanoparticles. The formation mechanism can be attributed to the weak laser penetration through the high mass ratio sucrose solution. This result illustrates that the critical parameters for the preparation of good cone arrays should be carefully controlled.

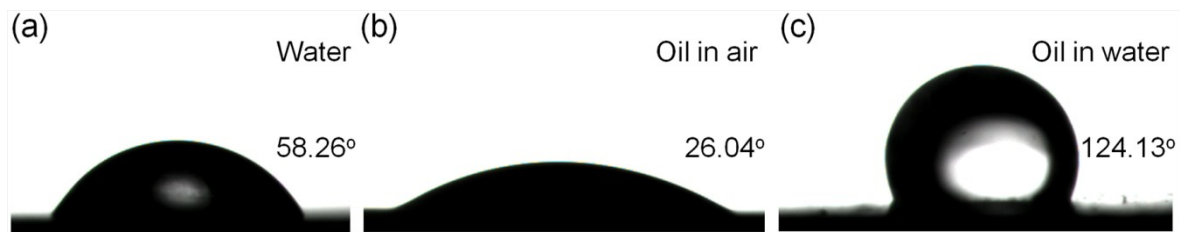


Figure S5. (a) The water contact state in air on flat nickel surface. The contact angle is 58.26° , declaring hydrophilic. (b) The oil contact state in air on flat nickel surface. Due to the low surface tension, the oil possesses contact angle of 26.04° , lower than that of water. (c) The oil contact model underwater on flat nickel surface. It is indicated that the hydrophilic flat nickel surface is tuned to oleophobic one when it is immersed in water, and the contact angle is 124.13° .

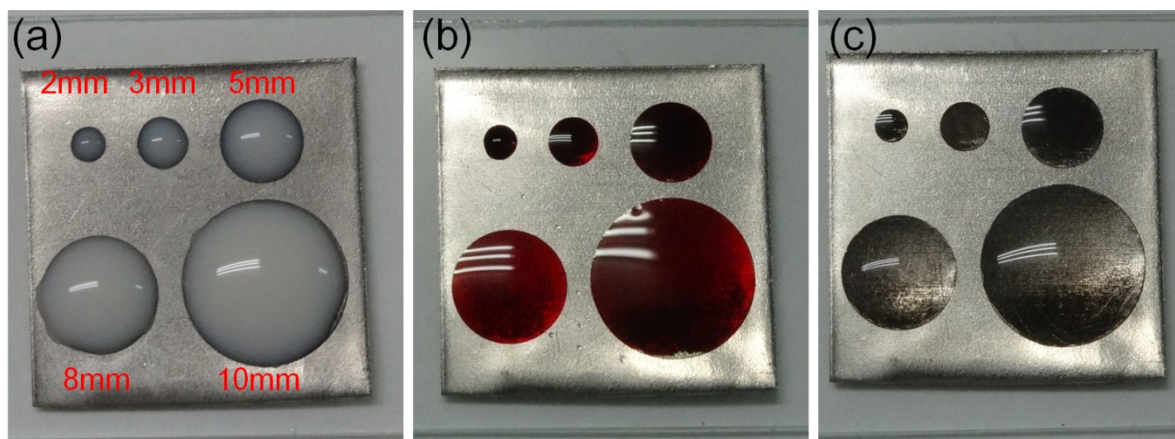


Figure S6. The static storage for (a) milk, (b) red ink and (c) oil with different dosage. The diameters of the designated area are 2, 3, 5, 8 and 10mm, respectively.

Supporting video 1. The rapid rolling of 5 μ l oil droplet on A surface. The rolling angle is about 2.2° . Due to the low adhesive force, the oil droplet rolls off the A surface very easily, and spends less than 0.75 s.

Supporting video 2. The rolling behavior of oil droplet on B surface. With the increase of adhesive force, the rolling angle for the same dosage oil is increased to 5.1° , and the sliding speed is lowered. The oil droplet rolls off the same distance with about 1 s.

Supporting video 3. The rolling behavior of oil droplet on C surface. Due to the enormous adhesive force, the oil droplet adheres to the C surface. When the surface is tilted about 9.9° , the oil droplet rolls off slowly, spending about 1.5 s.

Supporting video 4. The transportation dynamics of oil droplet along the set path. The red ink immediately flows along the set path once it contacts the starting point under the driving of extremely strong wicking force, rapidly travels over 50 mm in less than 6 s.